J IRAN CHEM SOC
DOI 10.1007/s13738-014-0539-y

ORIGINAL PAPER

Novel dye sensitizers of main chain polymeric metal complexes based on complexes of 2-(2′-pyridyl)benzimidazole derivative with Zn(II), Co(II): synthesis, characterization, and photovoltaic performance for dye-sensitized solar cells

Dahai Peng · Wei Zhang · Guipeng Tang · Jun Zhou · Jiaomei Hu · Qiufang Xie · Chaofan Zhong

Received: 11 January 2014 / Accepted: 27 June 2014

Abstract In this paper, four novel D–π–A polymeric metal complex as dye sensitizers for dye-sensitized solar cell, which have Poly(*p*-phenylenevinylene) or carbazole derivative used as an electron donor, thiophene derivatives used as π-bridge and 2-(2′-pyridyl)benzimidazole derivative metal (Zn, Co) complex used as an electron acceptor (A) were synthesized and characterized. They have been determined and studied by FT-IR, TGA, DSC, GPC, elemental analysis, UV–vis absorption spectroscopy, photoluminescence spectroscopy, cyclic voltammetry, J–V curves and IPCE plots. The results show that four novel polymeric metal complex exhibited good photovoltaic property and thermal stability. The DSSC fabricated by P1, P2, P3 and P4 exhibit good device performance with a power conversion efficiency of up to 2.15, 2.27, 2.30 and 2.41 % (under simulated air mass 1.5 G irradiation) respectively, indicating the polymeric metal complexes are promising in the development of DSSC.

Keywords Dye-sensitized solar cells · Polymeric metal complex · Power conversion efficiency · 2-(2’-pyridyl) benzimidazole · Carbazole · PPV

Introduction

Dye-sensitized solar cells (DSSC), also known as Grätzel cells, were invented by Grätzel and O’Regan in 1991 [1]. In comparison with the traditional silicon-based solar cells [2], dye-sensitized solar cells (DSSC) are one of the most promising power sources for a new generation of solar cells due to their energy-saving, versatile and environmental friendly nature. Among the key components of a DSSC, the sensitizer always plays as one of the most crucial elements since it exerts a significant influence on the power conversion efficiency (PCE) as well as the device stability. To date, the new method raises DSSC power conversion efficiency up to a record of 15 %, exceeding conventional, amorphous silicon-based solar cells [3].

There are various types of dyes which can be divided into metal-organic dyes [4–7], porphyrin dyes [8, 9], natural dyes and metal-free organic dyes [10–12] So far, Ru complexes dyes such as N3 [13], N719 [14], and black dye [15] as the most typical dyes have been used widely in the DSSC and the power conversion efficiencies of these Ru complexes dyes are up to over 11 % under air mass (AM) 1.5 illumination [16]. However, Ru complexes dyes met with some problems such as limited resources and difficult purification. Organic dyes as the promising alternative to Ru complexes dyes have been studied extensively due to their many advantages, diversity of molecular structures, high-molar extinction coefficient, low cost and environmental friendliness. Moreover, compared with small organic molecule, polymeric organic dyes show several advantages such as tunable band gaps and large absorption coefficients owing to its long conjugated chain, etc.

For the design of efficient molecular architectures, it is crucial to determine the energy levels of the three components of D–π–A sensitizers, as well as the location of the relevant orbitals within the D–π–A complex. Carbazole is a well-known electroluminescent and hole-transporting unit due to the electron-donating capabilities associated with the nitrogen in the carbazole. Wang and co-workers developed some organic dyes containing an N-aryl carbazole moiety

D. Peng · W. Zhang · G. Tang · J. Zhou · J. Hu · Q. Xie ·
C. Zhong (✉)
Key Laboratory of Environmentally Friendly Chemistry
and Applications of Ministry of Education, College of Chemistry,
Xiangtan University, Xiangtan 411105, Hunan, China
e-mail: zhongcf798@aliyun.com

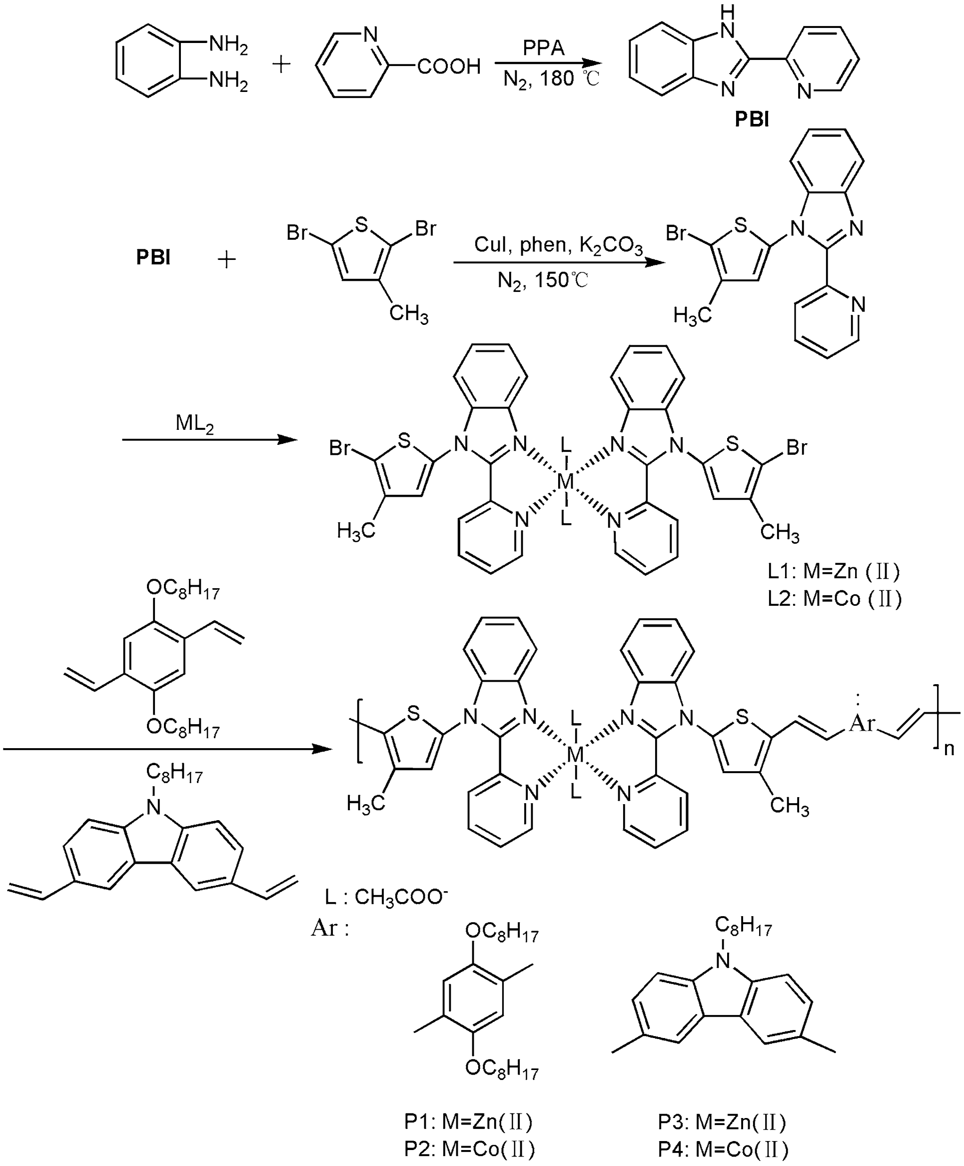

Scheme 1 Synthetic route of the monomers and polymeric metal complexes P1-P4

for DSSC and achieved a maximum conversion efficiency of 8.3 % under AM 1.5 G and a maximum IPCE value of 75 % at 470 nm [17]. Bridge groups, as electron spacers to connect the donor and acceptor, are not only to decide light absorption regions of the DSSC but also influence the electron injection from excited dyes to the TiO_2 surface. Thiophene and its derivatives have been successfully used as a π-conjugated bridge in the molecular design of organic dyes [18–20]. Benzimidazole and its derivatives are ubiquitous in biology. They have the larger π-conjugated system and the better electron donating property, it is significative to design and synthesize the polymeric complexes containing benzimidazole for improving electrochemical properties and thermal stability [21].

According to the above-mentioned points, we have designed and synthesized four D–π–A dyes possessing a metal-PBI as an acceptor (A), thiophene derivatives as a π-conjugation linkage (π) and PPV or CZ as donor group (D), which are shown in Scheme 1. Moreover, thermal properties, optical properties and photovoltaic properties of polymeric metal complexes are also investigated in this paper.

Experimental section

Materials

3-Methylthiophene and carbazole were obtained from Aldrich Chemical Co. and used as received. 1,4-bis(octyloxy)-2,5-divinylbenzene [22], N-octyl-3,6-divinyl -carbazole [23] and 2-(2’-pyridyl)benzimidazole was synthesized as previously reported [24]. N, N-dimethylformamide was dried by distillation over CaH_2 and methanol was dried over molecular sieves and freshly distilled prior to being used. The other materials were of common commercial grade and used as received. All chemicals used were of an analytical grade. Solvents were purified with conventional methods.

Instruments and measurements

^{1}H NMR spectra were obtained in $CDCl_3$ and recorded with a Bruker ARX400 (400 MHz) Germany and using tetramethylsilane (0.00 ppm) as the internal reference. FT-IR spectra were recorded using KBr pellets with a PerkinElmer Spectrum One FT-IR spectrometer over the range 400–4,000 cm^{-1}. Gel permeation chromatography (GPC) analyses were measured by a WATER 2414 system equipped with a set of HT_3, HT_4 and HT_5, l-styrayel columns with THF as eluent and polystyrene as standard. Thermogravimetric analyses (TGA), differential scanning calorimetry (DSC) and elemental analysis were performed on Shimadzu TGA-7 Instrument, Perkin-Elmer DSC-7 thermal analyzer and Perkin-Elmer 2400 II instrument, respectively. UV–visible spectra of all the polymers were taken on a Lambda 25 spectrophotometer. Photoluminescent spectra (PL) were taken on a Perkin-Elmer LS55 luminescence spectrometer with a xenon lamp as the light source. Cyclic voltammetry (CV) was conducted on a CHI630C electrochemical workstation using a three electrode system, in a $[Bu_4N]BF_4$ (0.1 M) DMF solution at a scan rate of 100 mV/s. The working electrode was a glassy carbon electrode, the auxiliary electrode was a platinum wire electrode and a saturated calomel electrode (SCE) was used as reference electrode.

Synthesis

Synthesis of 2-Bromo-5-[2-(2′-pyridyl)benzimidazolyl]-3-methylthiophene [25]

(PBI-Th).

A mixture of 2, 5-dibromo-3-methylthiophene (1.27 g, 5.0 mmol), 2-(2′-pyridyl)benzimidazole (0.99 g, 5.0 mmol), CuI (0.081 g, 0.43 mmol), 1,10-phenanthroline (0.16 g, 0.88 mmol) and K_2CO_3 (1.38 g, 8.9 mmol) was suspended in 3.0 mL of DMF. The mixture was refluxed for 24 h and then cooled to room temperature. The resulting brown sticky residue was extracted with CH_2Cl_2(50 mL × 4), and the organic extracts were combined, dried over $MgSO_4$ and purified by column chromatography (1:1 THF/hexane) to obtain the crude product of Brmt as yellow powder (0.74 g yield 40.2 %). ^{1}H NMR (400 MHz, $CDCl_3$): 8.57(s, 1H), 8.19(d, 1H), 7.86(d, 2H), 7.75–7.82(t, 1H), 7.40(s, 1H), 7.27(s, 2H), 6.78 (s, 1H), 2.23(s, 3H).

Synthesis of L1 [26]

$Zn(CH_3COO)_2 \cdot 2H_2O$ (0.22 g, 1 mmol) was dissolved in methanol (15 mL), and then *PBI-Th* (0.74 g, 2 mmol) in THF (20 mL) were added to the solution. Then 1 mol L^{-1} NaOH was added dropwise (under stirring) until the solution shows weakly acidic. After the solution was refluxed for 6 h, the reaction system was allowed to cool to room temperature. The precipitate was collected by filtration, washed with dried ether many times and then dried in vacuum at 60 °C. A yellow solid (0.42 g, yield 80 %) was obtained. FTIR (KBr; cm^{-1}): 3,095, 2,916 (aromatic and vinylic C–H), 1,650 (C = N), 1,483 (C = C), 1,150 (C–N–M), 510 (M–N). Anal. Calcd for $[C_{38}H_{30}Br_2N_6O_4S_2Zn]$: C, 49.39; H, 3.27; Br, 17.30; N, 9.10; O, 6.93; S, 6.94; Zn, 7.08; found: C, 49.05; H, 3.46; N, 8.75.

Synthesis of L2

In the same manner as described for L1, L2 affords a light brown solid (Yield: 91 %). Anal. Calcd for $C_{38}H_{30}Br_2N_6O_4S_2Co$: C, 49.74; H, 3.30; Br, 17.42; Co, 6.42; N, 9.16; O, 6.97; S, 6.99. Found: C, 49.23; H, 3.16; N, 9.24. FTIR (KBr, cm^{-1}): 3,068, 2,903 (aromatic and vinylic C–H), 1,663 (C = N), 1,475 (C = C), 1,116 (C–N–M), 504 (M–N).

Synthesis of Polymeric metal complex P1

The polymeric metal complex P1 was synthesized using the Heck coupling method, according to the literature [27]. A flask was charged with a mixture of metal complex L1 (0.173 g, 0.315 mmol), 1,4-bis(octyloxy)-2,5-divinylbenzene (0.122 g, 0.315 mmol), $Pd(OAc)_2$ (0.0024 g, 0.012 mmol), triethylamine (3 mL), 3-o-tolyl phospine (0.0220 g, 0.072 mmol) and DMF (8 mL). Then the flask was pumped into a vacuum and purged with N_2. The mixture was heated at 90 °C for 18 h under N_2. After that, it was cooled to room temperature and filtered, then the filtrate was poured into ethanol. The yellow precipitate was filtered and washed with cold ethanol. The crude product was purified by dissolving in DMF and precipitating into ethanol to afford a light yellow solid (Yield: 0.184 g, 53 %). FT-IR (KBr, cm^{-1}): 3,075, 2,930, 2,851, 1,658 (C = N), 1,052 (C–N–M), 475 (N–M). Anal. Calcd for $[C_{64}H_{70}N_6O_6S_2Zn]$: C, 67.24; H, 6.50; N, 7.13; O, 8.14; S, 5.44; Zn, 5.55. Found: C, 66.57; H, 6.32; N, 7.02. Mn = 7.8 kg/mol, PDI = 1.49.

Synthesis of Polymeric metal complex P2

With the similar synthetic method as P1, P2 affords solid (0.174 g, 51 %). FT-IR (KBr, cm^{-1}): 3,067, 2,915, 2,841, 1,675 (C = N), 1,096 (C–N–M), 496 (N–M). Anal. Calcd

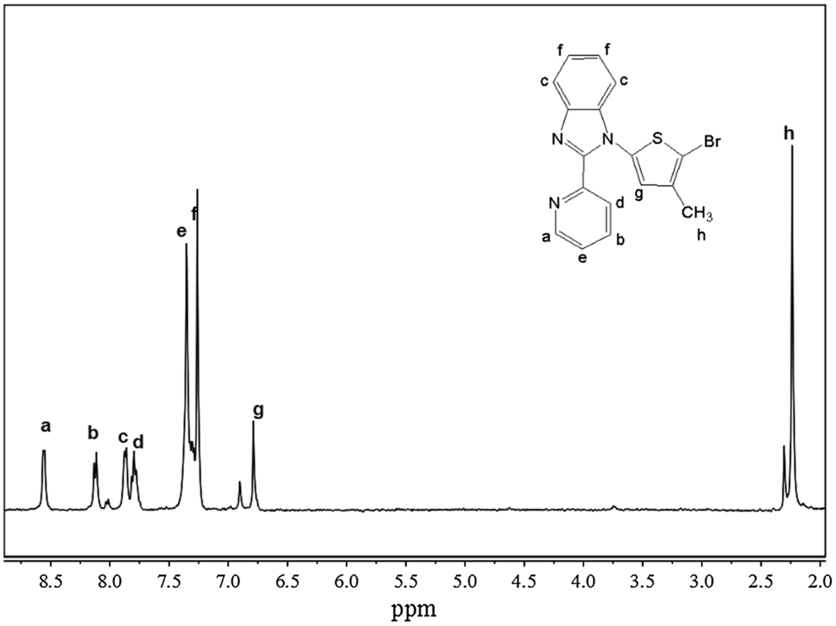

Fig. 1 ^{1}H NMR spectra of *PBI-Th* in $CDCl_3$ solution

for [$C_{64}H_{70}N_6O_6S_2Co$]: C, 67.61; H, 6.53; Co, 5.03; N, 7.17; O, 8.19; S, 5.47. Found: C, 67.23; H, 6.75; N, 7.11. Mn = 8.9 kg/mol, PDI = 1.63.

Synthesis of Polymeric metal complex P3

With the similar synthetic method as P1, P3 affords solid (0.195 g, 62 %). FT-IR (KBr, cm^{-1}): 3,086, 2,932, 2,854, 1,695 (C = N), 1,054 (C–N–M), 492 (N–M). Anal. Calcd for [$C_{62}H_{48}N_7O_4S_2Zn$]: C, 68.40; H, 5.65; N, 8.72; O, 5.70; S, 5.71; Zn, 5.82. Found: C, 68.03; H, 5.35; N, 8.71. Mn = 10.6 kg/mol, PDI = 1.54.

Synthesis of Polymeric metal complex P4

With the similar synthetic method as P1, P4 affords a yellow solid (0.168 g, 48 %). FT-IR (KBr, cm^{-1}): 3,076, 2,952, 2,844, 1,685 (C = N), 1,050 (C-N-M), 498 (N-M). Anal. Calcd for [$C_{62}H_{48}N_7O_4S_2Co$]: C, 68.80; H, 5.68; Co, 5.27; N, 8.78; O, 5.73; S, 5.74. Found: C, 68.03; H, 5.75; N, 8.71. Mn = 8.5 kg/mol, PDI = 1.51.

Results and discussion

Synthesis and characterization

The detailed synthetic routes of the four main chain polymeric metal complexes (P1, P2, P3, P4) are shown in Scheme 1, which were synthesized by the Heck coupling [28]. The four as-synthesized polymers could be dissolved in common organic solvents such as DMF at room temperature. But they exhibit a poor solubility in the other solvents, such as in methanol and chloroform.

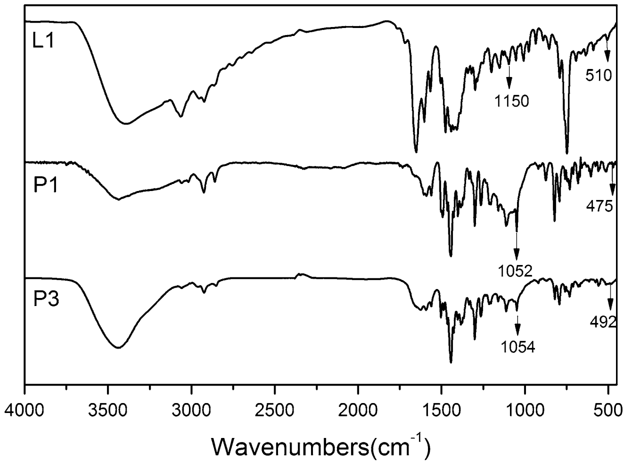

Fig. 2 FT-IR spectra of L1, P1, P3

Figure 1 displays the ^{1}H NMR spectrum of *PBI-Th*. In the ^{1}H NMR spectra of *PBI-Th* the proton signals at δ 8.57, 8.19, 7.86, 7.75 ~ 7.82, 7.40, 7.27, 6.78, 2.23 can be easily assigned to each corresponding hydrogen.

The IR spectra of the metal complex (L1, L2) and the target polymers (P1, P2, P3, P4) are shown in Figs. 2 and 3. From Figs. 2 and 3, absorption peaks at 1,616 cm^{-1} are due to C = N bond stretching vibration and 1,483 is the bond stretching vibration of C = C, the peaks of 1,150 cm^{-1} and 1,116 cm^{-1} are due to C–N–M stretching vibration of metal compound L1 and L2, respectively [29]. And then integrating with the results of elemental analysis, we can come up

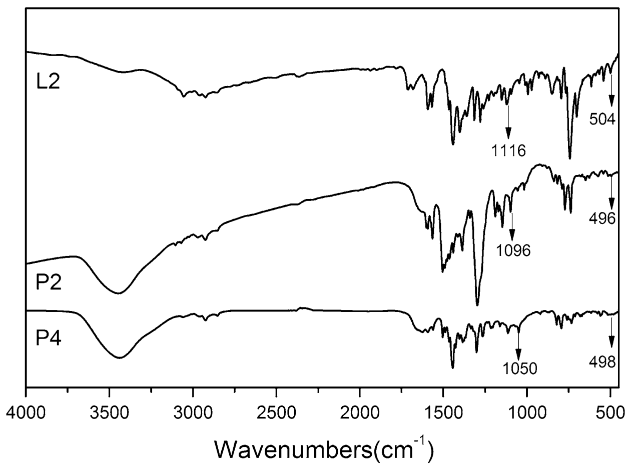

Fig. 3 FT-IR spectra of L2, P2, P4

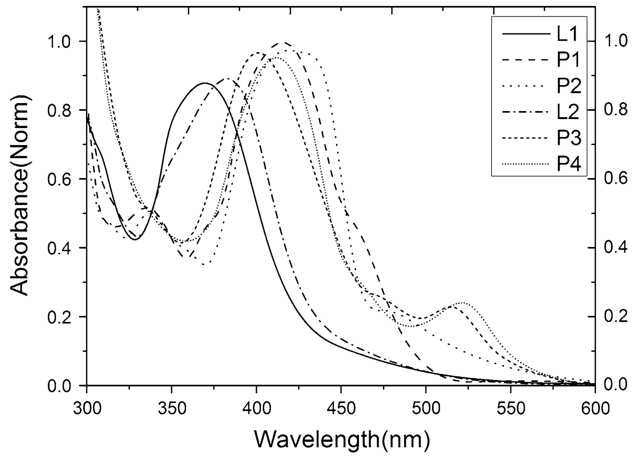

Fig. 4 UV-vis absorption spectra of L1, L2 and polymeric metal complexes P1-P4 in DMF solution

with the metals Zn^{2+} and Co^{2+} which have been successfully coordinated, namely, complexes L1 and L2 have been successfully synthesized.

Gel permeation chromatography (GPC) study for all the target polymers is shown in Table 1. The average molecular weight of P1, P2, P3 and P4 is 7.8, 8.9, 10.6 and 8.5 kg/mol and the units of them are 7, 8, 10 and 8, respectively. All the PDI of polymeric metal complexes are relatively wide (P1, P2, P3, P4: 1.49, 1.63, 1.54 and 1.51, respectively). The changes of the molecular weight also proved that the copolymerization has taken place between the monomers, which is a further evidence for the target polymers that have been successfully synthesized.

Optical properties

The UV–vis and normalized PL spectra of the polymeric metal complexes P1, P2, P3 and P4 (10^{-5} M in DMF solution and on TiO_2 film) are shown in Figs. 4, 5 and 6, respectively, and the corresponding data are summarized in Table 2.

The ligand L shows a UV–vis normalized absorption peak located at about 370 nm, corresponding to the π–π* electron transitions of the conjugated molecules. In Fig. 4, the maximum absorptions of P1, P2, P3 and P4 are at 422, 425, 416 and 424 nm, respectively. P3 and P4 polymers have very weak shoulder absorption peak in the band 520–550 nm due to the CZ of excellent electron-donating ability in the polymer. The one which shows a better UV absorption by comparing P2 with P4 as well as P1 with P3, indicates that polymers containing metal—Co have better absorption of light than polymers containing metal—Zn.

In UV–vis the maximum absorption peak of polymeric metal complexes P1, P2, P3 and P4 has a red-shift on TiO_2 film as shown in Fig. 5.

The normalized photoluminescent (PL) spectra of P1, P2, P3 and P4 in DMF solution are shown in Fig. 6 The excitation wavelengths were set according to the absorption peak of UV–vis spectrum and the corresponding optical data are also listed in Table 2. It can be seen that the PL peaks of them are at 471, 488, 467 and 475 nm, respectively, which can be attributed to the π–π* transition of intra-ligand.

Thermal stability

The thermal properties of the polymeric metal complexes were investigated by differential scanning calorimetric

Table 1 Molecular weights and thermal properties of the polymeric metal complexes

Polymer	$\bar{M}_n{}^a$ (× 10^3)	$\bar{M}_w{}^a$(× 10^3)	PDI	N	T_g^b (°C)	T_d^c(°C)
P1	7.8	11.6	1.49	7	173	335
P2	8.9	14.5	1.63	8	167	329
P3	10.6	16.3	1.54	10	194	373
P4	8.5	12.8	1.51	8	205	352

[a] Determined by gel permeation chromatography using polystyrene as standard

[b] Determined by DSC with a heating rate of 20 °C/min under nitrogen

[c] The temperature at 5 % weight loss under nitrogen

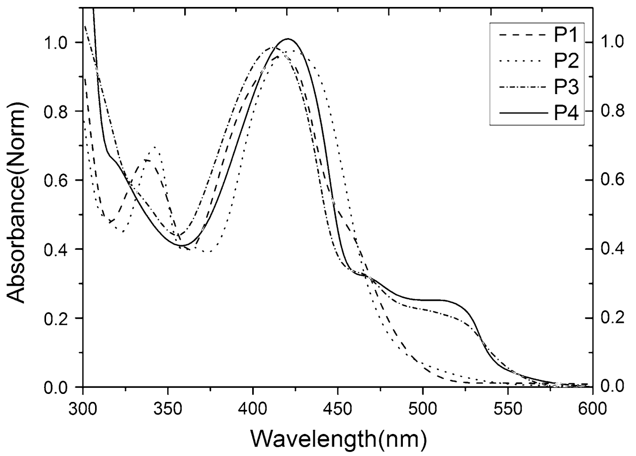

Fig. 5 UV-vis absorption spectra of polymeric metal complexes P1-P4 on TiO_2 film

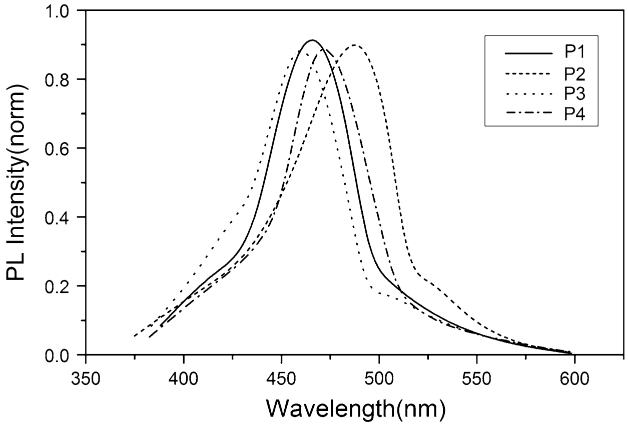

Fig. 6 PL spectra of the four polymeric metal complexes in DMF solution

(DSC) and thermo-gravimetric analysis (TGA) and the corresponding data are also reported in Table 1. The TGA image which is present in Fig. 7 shows that P1, P2, P3 and P4 possess good thermal stability with 5 % weight loss at temperatures (T_d) of 335, 329, 373 and 352 ºC in nitrogen, respectively. We could see that P1, P2, P3 and P4 have glass transition temperature (T_g) ranging from 167 to 105 ºC and followed the order P4 > P3 > P1 > P2, which suggests that polymeric metal complex containing CZ holds higher rigidity than that containing PPV.

Electrochemical properties

The electrochemical behaviors of the polymers were investigated by cyclic voltammetry, which is one of the important properties for organic materials used in solar cells. Figure 8 shows the cyclic voltammetry curves of P1, P2, P3 and P4. The lowest unoccupied molecular orbital (LUMO), highest occupied molecular orbital (HOMO) energy levels and energy gap (E_g) can be handled conveniently by equations as follows [30]:

$$\mathrm{HOMO} = \mathrm{e}(E_{ox} + 4.40)\ (\mathrm{eV})$$

$$\mathrm{LUMO} = -\mathrm{e}(E_{red} + 4.40)\ (\mathrm{eV})$$

$$E_g = \mathrm{HOMO} - \mathrm{LUMO}$$

The units of E_{ox} and E_{red} are measured through electrochemical curve and the data obtained are listed in Table 2. The reduction and oxidation potentials of P1 were measured to be E_{ox} = 1.12 V and E_{red} = –1.01 V, respectively. The energy value of the HOMO was calculated to be –5.52 eV and the energy value of the LUMO was calculated to be –3.39 eV, so the energy band gap was 2.13 eV. In the same way, we can get the related data of other polymers. The E_g of the complexes follows the order, P2 > P1 > P3 > P4, so P4 is more suitable for fabrication of optoelectronic devices than P1, P2 and P3, because a relatively low E_g can absorb light efficiently, it is very important to improve power conversion efficiency [31].

Table 2 Optical and electrochemical properties of the polymeric metal complexes

Polymer	$\lambda^{d}_{a,max}$, $\lambda_{a,onset}$	$\lambda^{e}_{p,max}$	E_{ox} (V)^g	E_{red} (V)^g	HOMO (eV)	LUMO (eV)	$E_{g,EC}$/eV ^{h}
P1	422,525	471	1.12	−1.01	−5.52	−3.39	2.13
P2	425,550	488	1.16	−1.07	−5.56	−3.33	2.23
P3	416,592	467	1.08	−0.97	−5.48	−3.43	2.05
P4	424,598	475	1.02	−0.99	−5.42	−3.41	2.01

[d] $\lambda_{a,max}$, $\lambda_{a,onset}$: The maxima and onset absorption from the UV–vis spectra in DMF solution

[e] $\lambda_{p,max}$: The PL maxima in DMF solution

[f] $E_{g,opt}$: Optical energy band gap calculated from the formula $E_g = 1{,}240/\lambda_{a,onset}$ (eV)

[g] Values determined by cyclic voltammetry

[h] $E_{g,EC}$: Electrochemical band gap estimated from HOMO and LUMO

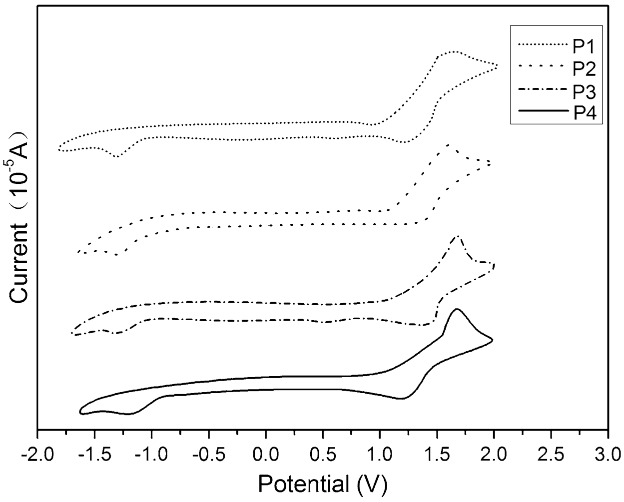

Fig. 7 TGA curves of P1-P4 with a heating rate of 20 °C/min under nitrogen atmosphere

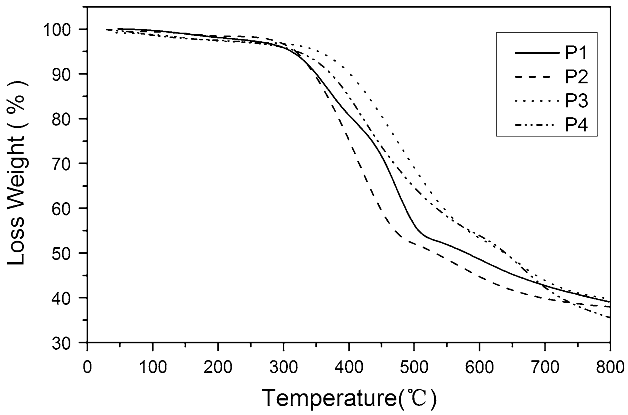

Fig. 8 Cyclic voltammograms for P1-P4 in DMF/0.1 M $[Bu_4N]BF_4$ at 100 mV/s

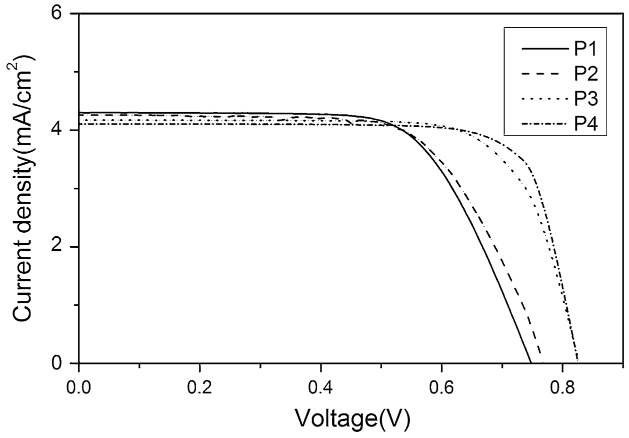

Fig. 9 J-V curves of DSSCs based on dyes (P1-P4) under the illumination of AM 1.5, 100 mW cm^{-2}

Table 3 Photovoltaic parameters of devices with sensitizers P1-P4 in DSSCs at full sunlight (AM 1.5 G, 100 wM cm^{-2})

Polymer	Solvent	J_{sc} (mA/cm^2)	V_{oc} (V)	*ff* (%)	η (%)
P1	DMF	4.32	0.75	66.4	2.15
P2	DMF	4.25	0.77	69.5	2.27
P3	DMF	4.22	0.82	67.3	2.30
P4	DMF	4.19	0.82	70.2	2.41

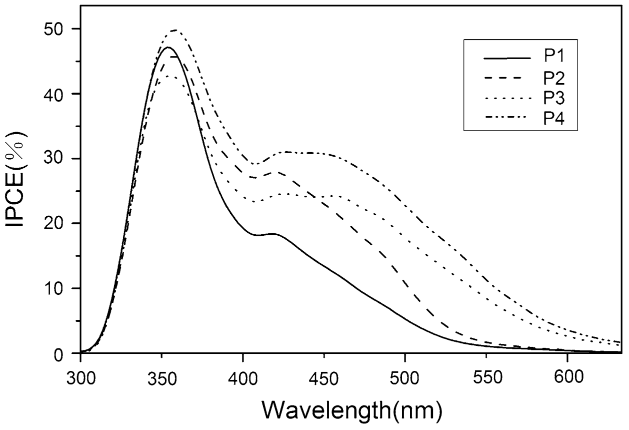

Fig. 10 Spectra of incident photon-to-current conversion efficiencies (IPCE) for DSSCs based on dyes (P1-P4)

Photovoltaic properties

Figure 9 displays the irradiation source for the photocurrent density–voltage (J–V) measurement of the DSSC devices based on the four polymeric metal complexes. Measurement of DSSC merits such as corresponding open-circuit voltage (V_{oc}), short-circuit current density (J_{sc}), fill factor (*ff*), and power conversion efficiency (η) are listed in Table 3. It can be seen from the table that the V_{oc} values of P1, P2, P3 and P4 are 0.75, 0.77, 0.82 and 0.82, respectively. The corresponding *ff* values could be achieved a higher level about 70.2 %. However, the J_{sc} values increased from 4.19 mA/cm^2 for P4 to 4.32 mA/cm^2 for P1. The power conversion efficiency based on P4 reached 2.41 %, which is the highest of the device based on those four polymeric metal complexes.

The low J_{sc} is chalked up to the long distance between donor and acceptor, which leads to the low charge separation and transportation efficiency and it also can be seen from the input photon to converted current efficiency (IPCE) curves as shown in Fig. 10. The IPCE values of P1, P2, P3 and P4 are only about 30 % at 425 nm, and are very low compared with N719 which could be achieved to 80 % at 425 nm [32]. As discussed in the UV–vis absorption spectra section, those two groups of data are proportional development and the IPCE value is decided by the absorption of light.

Conclusion

Four novel D–π–A polymeric metal complexes dyes comprising 2-(2′-pyridyl) benzimidazole derivative metal (Zn, Co) complex as the electron acceptor, thiophene derivatives as π-bridge and alkoxy benzene or carbazole derivative as electron donor were designed, synthesized and used for the fabrication of DSSC. The performance of the photovoltaic devices depended on the strength of the electron-donating group along the conjugated main. Among all of the dyes studied, DSSC based on P4 demonstrated the best overall light-to-electricity conversion efficiency of 2.41 % under AM1.5 irradiation. The results show that these polymeric metal complexes dyes are promising candidates in the development of high-performance DSSC.

As next work, there are still many challenges to obtaining outstanding PCE, especially the low J_{sc} based on the materials, narrow absorption spectra of the polymers and no adsorption affinities on the surface of TiO_2. For strong adsorption onto the surface of TiO_2, anchoring groups should also be introduced in the structure. This work provides a new path for the study and design of the new practical dye sensitizers.

References

1. B. O'Regan, M. Grätzel, Nature **353**, 737 (1991)
2. N. Lior, Energy. **33**, 842 (2008)
3. J. Burschka, N. Pellet, S. Moon, R. Humphry-Baker, P. Gao, K. Mohammad Nazeeruddin, M. Grätzel, Nature. **499**, 316–319 (2013)
4. M. Ishida, S.W. Park, D. Hwang et al., J. Phys. Chem. **C115**, 19343 (2011)
5. C.Y. Lin, C.F. Lo, L. Luo et al., J. Phys. Chem. **C113**, 755 (2009)
6. D.W. Chang, S.J. Ko, Y.K. Jin et al., Macromol. Rapid Commun. **32**, 180 (2011)
7. Z.S. Wang, N. Koumura, Y. Cui et al., Chem. Mater. **20**, 3993 (2008)
8. M. Ishida, S.W. Park, D. Hwang et al., J. Phys. Chem. **C115**, 19343 (2011)
9. C.Y. Lin, C.F. Lo, L. Luo et al., J. Phys. Chem. **C113**, 755 (2009)
10. D.W. Chang, S.J. Ko, Y.K. Jin et al., Macromol. Rapid Commun. **32**, 180 (2011)
11. Z.S. Wang, N. Koumura, Y. Cui et al., Chem. Mater. **20**, 3993 (2008)
12. Z. Fang, A.A. Eshbaugh, K.S. Schanze et al., J. Am. Chem. Soc. **133**, 3063 (2011)
13. M. Grätzel, J. Photochem. Photobiol., A **168**, 235 (2004)
14. M.K. Nazeeruddin, A. Kay, L. Rodicio, R. Humphry-Baker, E. Mu¨ller, P. Liska, N. Vlachopoulos, M. Grätzel, J. Am. Chem. Soc. **115**, 6382 (1993)
15. M.K. Nazeeruddin, P. Pechy, T. Renouard, S.M. Zakeeruddin, R. Humphry-Baker, P. Comte, P. Liska, L. Cevey, E. Costa, V. Shklover, L. Spiccia, G.B. Deacon, C.A. Bignozzi, M. Grätzel, J. Am. Chem. Soc. **123**, 1613 (2001)
16. L.Y. Lin, C.H. Tsai, K.T. Wong, T.W. Huang et al., J. Org. Chem. **75**, 4778 (2010)
17. Z.S. Wang, N. Koumura, Y. Cui, M. Takahashi, H. Sekiguchi, A. Mori, T. Kubo, A. Furube, K. Hara, Chem. Mater. **20**, 3993 (2008)
18. R. Chen, X. Yang, H. Tian, L.J. Sun, Photochem. Photobiol. A: Chem. **189**, 295–300 (2007)
19. N. Koumura, Z. Wang, S. Mori, M. Miyashita, E. Suzuki, K.J. Hara, Am. Chem. Soc. **130**, 4202–4203 (2008)
20. H. Choi, C. Baik, S.O. Kang, J. Ko, M.S. Kang, M.K. Nazeeruddin, M. Grätzel, Angew. Chem. Int. Ed. **47**, 327–330 (2008)
21. C.F. Zhong, A.H. He, R.F. Guo, Q. Wu, H.L. Huang, Synth. Met. **158**, 33–37 (2008)
22. K. Liu, Y. Li, M.J. Yang, J. Appl. Polym. Sci. **111**, 1976 (2009)
23. Jean-Francois Morin, Nicolas Drolet, Ye Tao, Mario Leclerc, Chem. Mater. **16**, 4619–4626 (2004)
24. E. Alcalde, I. Dinare´s, L.P. Grcia, Synthesis (1992) 395
25. Qin-De Liu, Wen-Li Jia, Suning Wang, Inorg. Chem. **44**, 1332–1343 (2005)
26. L.F. Xiao, Y. Liu, Q. Xiu, L. Zhang, L. Guo, H. Zhang, C.F. Zhong, Tetrahedron **66**, 2835–2842 (2010)
27. L.R. Tsai, Y. Chen, J. Polym. Sci. Part A: Polym. Chem. **46**, 70–84 (2008)
28. C. Ziegler, R. Heck, J. Org. Chem. **43**, 2941–2946 (1978)
29. Y. Liu, Q. Xiu, L. Xiao, H. Huang, L. Guo, L. Zhang, H. Zhang, S. Tan, C. Zhong, Polym. Adv. Technol. **22**, 2583 (2011)
30. X.Z. Li, W.J. Zeng, Y. Zhang, Q. Hou, W. Yang, Y. Cao, Eur. Polym. J. **41**, 2923 (2005)
31. Y.J. Cheng, S.H. Yang, C.S. Hsu, Chem. Rev. **109**, 5868 (2009)
32. F. Odobel, E. Blart, M. Lagre´e, M. Villieras, H. Boujtita, N.E. Murr, S. Caramori, C.A. Bignozzi, J Mater Chem. **13**, 502–510 (2003)